PCCP

View Online
Dynamic Article Links

Cite this: *Phys. Chem. Chem. Phys.*, 2011, **13**, 18330–18338

www.rsc.org/pccp

PAPER

Double ionization of cycloheptatriene and the reactions of the resulting $C_7H_n^{2+}$ dications (n = 6, 8) with xenon†

Daniela Ascenzi,*[a] Julia Aysina,[a] Emilie-Laure Zins,[bc] Detlef Schröder,*[b] Jan Žabka,[d] Christian Alcaraz,[ef] Stephen D. Price[g] and Jana Roithová*[h]

Received 21st May 2011, Accepted 11th July 2011
DOI: 10.1039/c1cp21634a

The formation and fragmentation of the molecular dication $C_7H_8^{2+}$ from cycloheptatriene (CHT) and the bimolecular reactivities of $C_7H_8^{2+}$ and $C_7H_6^{2+}$ are studied using multipole-based tandem mass spectrometers with either electron ionization or photoionization using synchrotron radiation. From the photoionization studies, an apparent double-ionization energy of CHT of (22.67 ± 0.05) eV is derived, and the appearance energy of the most abundant fragment ion $C_7H_6^{2+}$, formed *via* H_2 elimination, is determined as (23.62 ± 0.07) eV. Analysis of both the experimental data as well as results of theoretical calculations strongly indicate, however, that an adiabatic transition to the dication state is not possible upon photoionization of neutral CHT and the experimental value is just considered as an upper bound. Instead, an analysis *via* two different Born–Haber cycles suggests ^2IE(CHT) = (21.6 ± 0.2) eV. Further, the bimolecular reactivities of the $C_7H_n^{2+}$ dications (n = 6, 8), generated *via* double ionization of CHT as a precursor, with xenon as well as nitrogen lead, *inter alia*, to the formation of the organo-xenon dication $C_7H_6Xe^{2+}$ and the corresponding nitrogen adduct $C_7H_6N_2^{2+}$.

1. Introduction

Until a few years ago, small or medium-sized molecular dications were by and large considered to only afford either electron- or proton transfer reactions with neutral reagents,[1,2] while bond forming reactions were limited to a very few exceptions to this rule.[3–5] Starting from our first observation in 2006,[6] we found, however, that hydrocarbon dications $C_mH_n^{2+}$, and related species, have their "own" chemistry in which they act as superelectrophiles and yet can undergo bond-forming with maintenance of the two-fold charge.[7–15] The high reactivity of these gaseous dications allows their reaction with inert species (*e.g.* CO_2, N_2)[16,17] or even rare gases.[18–23] Only recently, we have investigated the reactions of xenon with $C_7H_n^{2+}$ dications (n = 6–8) generated by double ionization of toluene.[23] Here, we compare these results with those obtained when the isomeric cycloheptatriene (CHT) molecule is used as the neutral precursor. The objectives of this comparative study are to probe if different neutral precursors allow specific access to different parts of the rather complex potential-energy surface (PES) which arises from double ionization of toluene.[24,25] Specifically, the toluene structure is only a shallow minimum on the $C_7H_8^{2+}$ PES and it can easily undergo hydrogen migration to ring-protonated tautomers of the benzylium cation or experience a ring-expansion to the CHT dication. In conjunction with energy-resolved photoionization studies using synchrotron radiation, these measurements could experimentally map out the $C_7H_8^{2+}$ potential-energy surface, thereby possibly providing a benchmark for the energetics of medium-sized hydrocarbon dications. As shown below, however, it turns out that understanding the double ionization of neutral CHT poses a formidable challenge in its own right.

2. Experimental and theoretical details

The photoionization experiments were performed with the CERISES apparatus[26–28] which was installed on the DESIRS

[a] *Department of Physics, University of Trento, Via Sommarive 14, 38123 Povo, Italy*
[b] *Institute of Organic Chemistry and Biochemistry, Academy of Sciences of the Czech Republic, Flemingovo náměstí 2, 16610 Prague 6, Czech Republic*
[c] *Laboratoire de Dynamique, Interactions et Réactivité, UMR 7075 CNRS/UPMC, Université Pierre et Marie Curie, 4 Place Jussieu, 75252 Paris Cedex 05, France*
[d] *J. Heyrovský Institute of Physical Chemistry, Academy of Sciences of the Czech Republic, Dolejškova 3, 18223 Prague 8, Czech Republic*
[e] *Laboratoire de Chimie Physique, Bât. 350, UMR 8000, CNRS – Univ. Paris-Sud 11, Centre Universitaire Paris-Sud, 91405 Orsay Cedex, France*
[f] *Synchrotron SOLEIL, L'Orme des Merisiers, Saint-Aubin – BP 48, 91192 Gif-sur-Yvette, France*
[g] *University College London, Department of Chemistry, 20 Gordon Street, London WC1H 0AJ, UK*
[h] *Department of Organic and Nuclear Chemistry, Faculty of Science, Charles University in Prague, Hlavova 8, 12843 Prague 2, Czech Republic*

† Electronic supplementary information (ESI) available. See DOI: 10.1039/c1cp21634a

beamline of the synchrotron radiation source SOLEIL (France). This beamline provides monochromatic photons in the range of 5–40 eV by using three different gratings. In the present experiments, the resolution was set to $E/\Delta E = 500$ in the photon-energy range from 20 to 28 eV, *i.e. ca.* 50 meV at E(photon) = 25 eV. The photon energy was calibrated with accuracy better than ±5 meV by measuring the ionization energy of argon around 15.76 eV and the $3s3p^6np$ (n = 5–9) window resonances in the Ar^+ yield between 28 and 29 eV. Samples were introduced *via* a gas inlet, ionized by photons, and the resulting dications were extracted by a field of 1 V cm^{-1} towards a QOOQ system (Q stands for quadrupole and O for octopole). The photon energy was scanned in steps of 25 meV. For the determination of photoionization thresholds, Q2 was used to mass-select the ions of interest, while Q1, O1, and O2 just served as ion guides; use of the last mass analyzer (Q2) helps to minimize the kinetic shift in dissociative ionization. We can estimate that, under our operative conditions, the flight time of a dication from the source to the entrance of Q2 is about 500 μs. In the reactive monitoring experiments[29–31] described below in more detail, the precursor ion was mass-selected using Q1, while Q2 was set to the mass of the product ion and the photon energy was scanned. Ions were detected by a multi-channel plate operating in the counting mode. During the measurements of the ion yields, electron yields were also simultaneously recorded as well as photon fluxes, which were monitored by photoemission currents from a gold grid. The electron yield helps in monitoring, and correcting for, fluctuations of the pressure in the source. The raw data for the measured ion yields were corrected for the photon flux of the beam line as a function of photon energy.

Most ion/molecule reactions were investigated in a home-built guided-ion beam apparatus of the Trento team, which consists of a tandem mass spectrometer with an OQOQ configuration.[32,33] Ions are generated by electron ionization (EI) of cycloheptatriene at energies in the range of 70–100 eV. The first octopole O1 is operated as an ion guide. The quadrupole Q1 acts as a mass filter to select the $C_7H_n^{2+}$ parent dications at m/z 45.0 for n = 6, m/z 45.5 for n = 7, and m/z 46.0 for n = 8, respectively. The parent ions are injected into O2 which is surrounded by a scattering cell filled with the desired neutral reactant, the pressure of which is monitored by a spinning rotor gauge. The kinetic energy of the projectile ion-beam, which determines the collision energy between the parent ions and rare gas molecules, can be varied from about 0 to 100 eV by changing the bias potential of O2. Product ions are mass analyzed by Q2 and detected by an electron multiplier.

Electronic structure calculations to interpret the experimental results were performed using the density functional method B3LYP[34–37] in conjunction with the 6-311+G(2d,p) basis sets[38,39] as implemented in the Gaussian 03 suite.[40] For all optimized structures, frequency analyses at the same level of theory were used in order to assign them as genuine minima or transition structures on the PES as well as to calculate zero-point vibrational energies (ZPVEs). Transition structures were further characterized by intrinsic reaction coordinate (IRC) calculations.[41,42] The relative energies (E_{rel}) of the structures given below refer to energies at 0 K and are anchored to $E_{rel}(C_6H_5–CH_3 + Xe) = 0.00$ eV, where $C_6H_5–CH_3$ stands for toluene; for related isomers of $C_7H_8^{2+}$ as well as $C_7H_8Xe^{2+}$, see ref. 23 and 25, in which the PESs relevant to the rearrangements of the various associated isomers $C_7H_8^{2+}$ and their adducts with xenon are described.

3. Results and discussion

Accompanying much more intense monocation signals, electron ionization of CHT at a nominal electron energy of 100 eV gives rise to a series of $C_7H_n^{2+}$ dications, of which the most abundant corresponds to the dehydrogenated molecular dication $[M - H_2]^{2+}$ ($C_7H_6^{2+}$, m/z 45), followed by the molecular dication $C_7H_8^{2+}$ with m/z 46, and a dication formed by loss of atomic hydrogen (*i.e.* $C_7H_7^{2+}$ at m/z 45.5). In the representative mass spectrum shown in Fig. 1, the relative ratios of $C_7H_6^{2+}$, $C_7H_7^{2+}$, and $C_7H_8^{2+}$ are *ca.* 100 : 35 : 50, while the hydrogen-depleted species such as $C_7H_5^{2+}$ and $C_7H_4^{2+}$ appear in much smaller abundances. We note that the dication region in the EI spectrum of isomeric toluene reveals formation of analogous dications, but the respective abundances differ. Especially, the abundance of H_2 loss relative to the intensity of the parent dication is smaller for toluene compared to CHT.

3.1 Double photoionization of cycloheptatriene

To achieve some specific insight into the dication energetics, we determined the phenomenological appearance threshold for double photoionization of CHT using synchrotron radiation. Fig. 2 shows the yields of the molecular dication $C_7H_8^{2+}$ and of the primary fragment $C_7H_6^{2+}$, formed *via* dehydrogenation of $C_7H_8^{2+}$, in the photon-energy range from 21.5 to 27 eV. Unlike several previous cases,[11,13,23] above the apparent photoionization threshold at about 23 eV, the ion yield of the parent dication $C_7H_8^{2+}$ shows an approximately linear dependence with increasing photon-energy.

The double ionization energy of an atom or a molecule (^2IE) can be extracted from the photoion appearance curve in several ways. The classical approach is based on an extrapolation of the linear part of the rise of the total dication yield

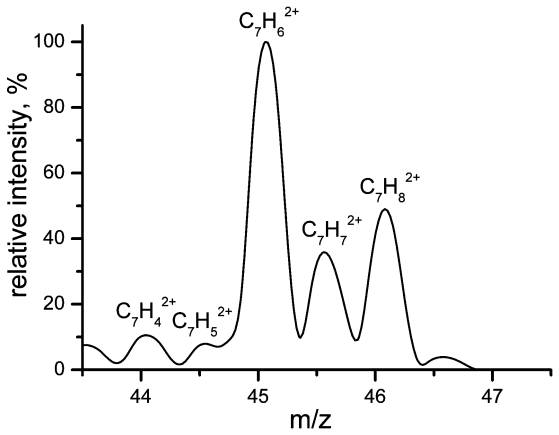

Fig. 1 Relative yields of the $C_7H_n^{2+}$ dications produced by electron ionization of neutral cycloheptatriene at a nominal electron energy of 100 eV.

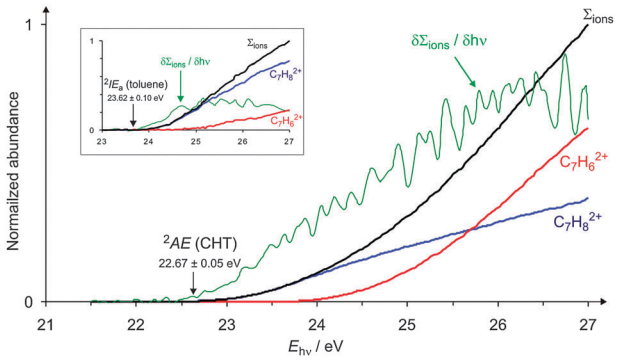

Fig. 2 Photoionization threshold for the double ionization of CHT with synchrotron photons in the region from 21.5 to 27 eV to afford the molecular dication $C_7H_8^{2+}$ and the dehydrogenated dication $C_7H_6^{2+}$ as well as their sum (labeled as Σ_{ions}). The noisy line (labeled as $\delta\Sigma_{ions}/\delta h\nu$) shows the first derivative of Σ_{ions} as a function of the photon energy. The data are the average of three independent photon-energy scans. The inset shows the corresponding data obtained using toluene as a neutral precursor which was acquired in the same synchrotron session (single scan). See main text for an explanation of the notations ^2IE and ^2AE.

(Σ_{ions}) to the baseline, but this method often overestimates ^2IE significantly due to the neglect of Franck–Condon effects. In the case of toluene, explicit consideration of the Franck–Condon envelope in fact led to a revision of its ^2IE by almost 1 eV,[24] which has independently been confirmed by photoelectron–photoion coincidence measurements.[43] However, this procedure involves the explicit consideration of all possible rovibrational states involved and is therefore rather demanding. In subsequent work, we used the analogy to single photoionization and suggested the determination of ^2IE by extrapolation of the rise of the first derivative of Σ_{ions} to the baseline ("derivative method").[44,45] According to the Wannier laws for photoionization,[46–50] the first derivative of Σ_{ions} should show a sigmoid shape, rapidly reaching a plateau. In a related variant, a model curve having the shape of the Franck–Condon envelope is directly fitted to the raw ionization data, a fit which requires some assumptions, but is preferred over the derivative method for poorer data sets.[13,51] To illustrate the derivative method, the inset in Fig. 2 shows data for the double ionization of toluene obtained in the same beam time session as those for CHT. The derivative (indicated by a vertical arrow in the inset) shows the expected sigmoid shape and extrapolation of the initial rise to the baseline matches the literature value of ^2IE(toluene) = (23.62 ± 0.1) eV reasonably well.

In marked contrast, the derivative of Σ_{ions} in the case of CHT continuously increases from an apparent onset at about 22.5 eV over a range of several eV and a plateau-type behavior could only be assigned somewhere above 26 eV; note in this context that the Wannier law is generally assumed to hold only up to 2 eV above threshold.[52,53] Linear extrapolation of the derivative over various energy regimes between 22.5 and 26 eV leads to an average of ^2AE(CHT) = (22.67 ± 0.05) eV, however, we refrain from a conversion of this number into ^2IE(CHT) at this point and next turn to the discussion of thermochemistry and theory. As far as dehydrogenation is concerned, to a first approximation an estimate for the energy required to afford the $C_7H_6^{2+}$ fragment can be obtained by horizontal shifting of the curve of the sum of ions (Σ_{ions}) until it matches that of $C_7H_6^{2+}$.[23] Within the energy range shown, a good overlap of both curves is obtained for a shift of ΔE_{shift} = (0.95 ± 0.05) eV, which hence converts into $AE(C_7H_6^{2+}{}_{CHT})$ = (23.62 ± 0.07) eV for dissociative double ionization of CHT into $C_7H_6^{2+}$. In comparison, the corresponding value of $AE(C_7H_6^{2+}{}_{Tol})$ = (25.2 ± 0.1) eV[54] is obtained by applying the same method for the determination of the appearance energy of $C_7H_6^{2+}$ upon dissociative double ionization of toluene.[23] Note that the difference of 1.42 eV in the heats of formation of CHT and toluene has to be acknowledged,[55] which leads to a relative energy of (25.04 ± 0.1) eV of the $C_7H_6^{2+}$ ion generated from neutral CHT relative to the energy of neutral toluene. The values obtained for the $C_7H_6^{2+}$ fragment therefore agree quite well and support the previous conclusion that dehydrogenation of the toluene dication is associated with ring expansion to afford the corresponding cycloheptatrienylidene dication.[23,25]

In the corresponding Born–Haber cycle summarizing the energetics (Scheme 1), two energies (in grey) are given for the energy of the CHT^{2+} dication. The lower value (22.92 eV) is derived from the experimental ^2IE of toluene using the computed energy difference of 0.70 eV between the toluene

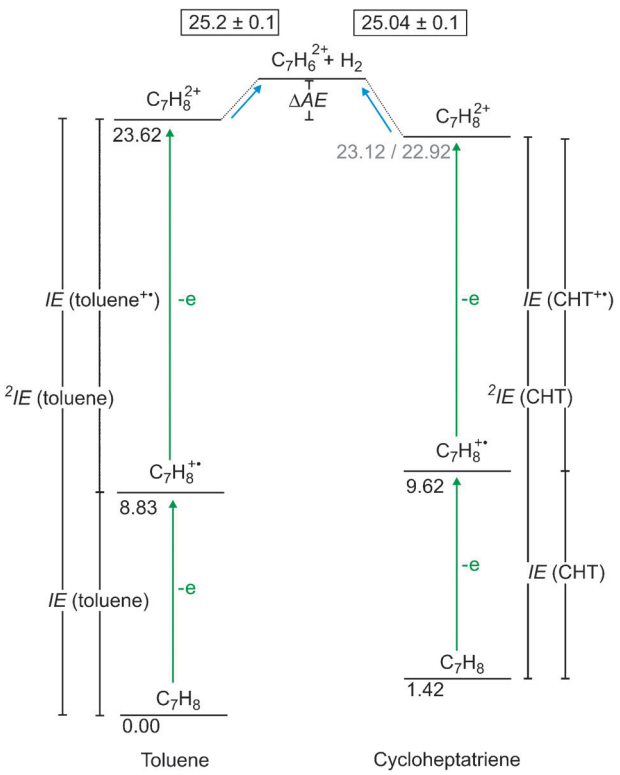

Scheme 1 Born–Haber cycle connecting the neutral, mono- and dicationic states of toluene and cycloheptatriene, respectively. Energies are given in eV relative to neutral toluene. The grey values for the CHT dication are derived from theory (see text). The numbers on top in the rectangular boxes are the energies of the $C_7H_6^{2+}$ dications as derived from experimental appearance energies of $C_7H_6^{2+}$ from double photoionization of toluene (left) and CHT (right).

Table 1 Selected single and double ionization energetics (adiabatic values at 0 K in eV) for the C_7H_8 isomers of toluene and cycloheptatriene calculated at the B3LYP/6-311+G(2d,p) level of theory

	Toluene		Cycloheptatriene	
	Exp.	Calc.	Exp.	Calc.
$IE(C_7H_8)$	8.828 ± 0.001[55]	8.58	8.20 ± 0.05[55]	7.74
$IE(C_7H_8^{+\bullet})$	14.8 ± 0.1[24]	14.56		13.21
$^2IE(C_7H_8)$	23.62 ± 0.1[24,43]	23.14		20.95
$\Delta H_{f,rel}(C_7H_8)^a$	0.00	0.00	1.42[55]	1.49
$AE(C_7H_6^{2+})$	25.2 ± 0.1	24.36[b]	23.62 ± 0.07	22.87

[a] Value given relative to neutral toluene, the absolute heat of formation of toluene is (0.52 ± 0.01) eV.[55] [b] Value refers to dehydrogenation affording the more stable cycloheptatrienylidene dication.

$C_7H_8^{2+}$ dication and the isomeric CHT^{2+} dication.[25] The slightly larger value (23.12 eV) is calculated from the appearance energy of $C_7H_6^{2+}$ from CHT in conjunction with the computed endothermicity of 1.92 eV for the loss of molecular hydrogen from CHT^{2+} (see below). Together with the relative energy of neutral CHT, these values imply ^2IE(CHT) = 21.50 and 21.70 eV, respectively, whereas the experimental value derived from the photoionization experiments, ^2AE(CHT) = (22.67 ± 0.05) eV is about 1 eV higher in energy. In order to understand this seemingly large discrepancy, we have performed a series of quantum chemical calculations which are discussed below.

In general, the density functional theory calculations reproduce the experimental energetics reasonably well (Table 1), although theory systematically underestimates the ionization energies by 0.1–0.4 eV. For a given charge state, however, the deviations are smaller, *e.g.* the energy difference between neutral toluene and neutral CHT is predicted with an error of only 0.07 eV compared to the literature values. Also as far as the dications are concerned, the computed energy demand of 1.22 eV for the dehydrogenation of the toluene dication to the energetically more stable cycloheptatrienylidene dication compares reasonably well with the experimental value of 1.6 ± 0.1 eV.[23] Accordingly, despite the underestimated ionization energies, the computed ^2IE(CHT) = 20.95 eV is in obvious disagreement with the assumption that ^2IE(CHT) would correspond to the experimentally determined value ^2AE(CHT) = (22.67 ± 0.05) eV (Fig. 2).

The origin of this discrepancy lies in the vertical nature of the photoionization process (Fig. 3). While in the case of toluene, the difference between the vertical and adiabatic ionization $\Delta^2IE_{v/a}$(toluene) amounts to 1.02 eV, this value amounts to 1.76 eV in the case of CHT. With such a large difference it is fair to assume that the 0 → 0 transition from neutral CHT to the corresponding dication has a negligible intensity. Consequently, the photoionization to the dication will not show a threshold at the adiabatic ^2IE, but at a value being higher in energy to a significant but unknown extent. This rationale also explains the unusual shape of the photoionization cross section for forming the dications, shown in Fig. 2 and the deviation of the first derivative from the expected sigmoid shape. Accordingly, the value ^2AE = (22.67 ± 0.05) eV in Fig. 2 can only be regarded as an upper limit of ^2IE(CHT), because CHT appears to be a case in which

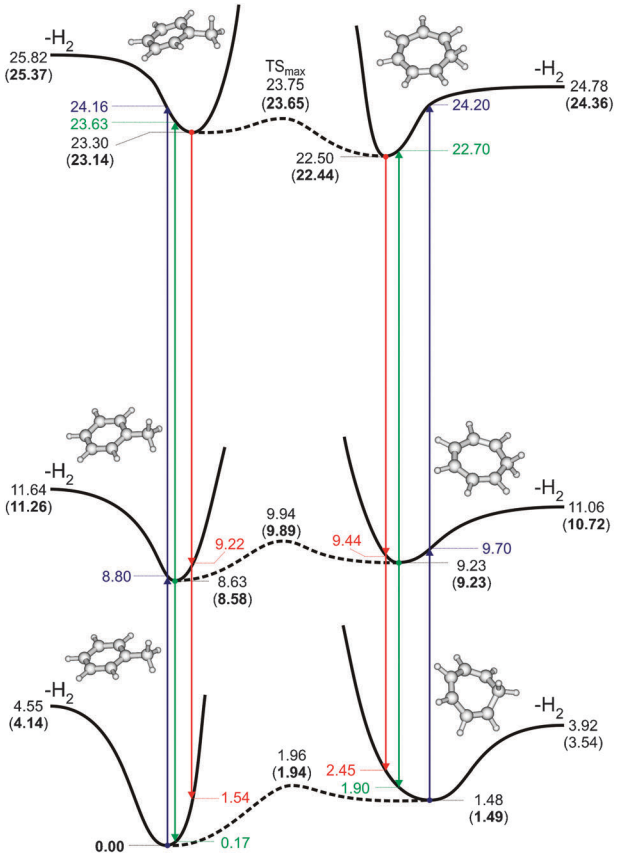

Fig. 3 Summary of the computed energetics of the neutral, mono- and dicationic states of toluene and cycloheptatriene, respectively, and the energies of the corresponding vertical transitions from the respective minima (indicated by dots) *via* either vertical ionization from neutrals (indicated by consecutive upward arrows starting from the minima of the neutral), vertical recombination from dications (indicated by consecutive downward arrows starting from the minima of the dications) and either vertical ionization or recombination from monocations (indicated by upward and downward arrows starting from the minima of the monocation); adiabatic energies are in black. In order to allow a direct comparison with the Born–Haber cycle shown in Scheme 1, all energies are given in eV relative to neutral toluene. The energies are derived from total electronic energies. The bold values in brackets are energies corrected with zero-point vibrational energy and correspond to the values listed in Table 1. The dissociation channels for the different charge states of toluene refer to 1,1-dehydrogenations from the methyl group to afford the corresponding phenylcarbene in the respective charge states, and those for cycloheptatriene correspond to the 1,1-eliminations to yield the respective charge states of cycloheptatrienylidene.

the adiabatic ionization from the neutral to the dication is rather improbable. We note in passing that in the case of CHT, the triplet state of the molecular dication is too high in energy (adiabatically 1.56 eV above the singlet ground state)[25] to significantly contribute to the photoionization cross section near the adiabatic threshold.

Summarizing the results of the Born–Haber cycle which includes both the experimental findings and theoretical results, in this exceptional case of hydrocarbon photoionization we assign the adiabatic second ionization energy of cycloheptatriene as ^2IE(CHT) = (21.6 ± 0.2) eV, where the increased

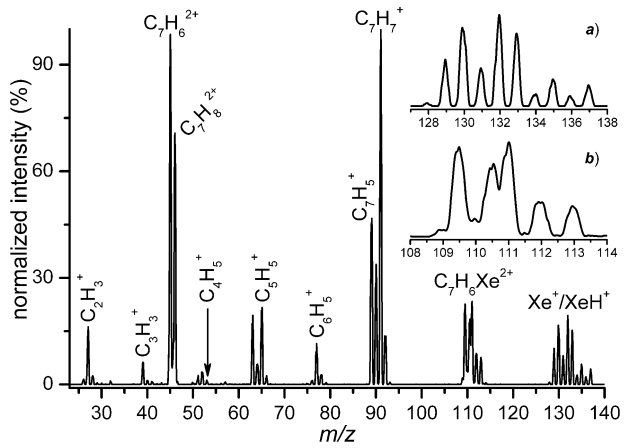

Fig. 4 Reaction of the mass-selected $C_7H_8^{2+}$ dication generated from dissociative electron ionization of CHT with Xe (at a pressure of about 3×10^{-3} mbar in the reaction cell) at a nominal collision energy E_{CM} = 1.1 eV. The insets (a) and (b) show the mass regions of Xe^+/XeH^+ and the $C_7H_6Xe^{2+}$ products on expanded scales. Note that the xenon pressure applied is well above single collision conditions.

error bar should cover the remaining uncertainty in the analysis of both the experimental data and the theoretical predictions.

3.2 Guided ion beam experiments

In analogy to our previous work on $C_7H_n^{2+}$ dications (n = 6, 8) formed from toluene,[23] we probed the reactions of xenon with these dications generated *via* double ionization of neutral CHT. Fig. 4 shows the mass spectrum obtained upon reaction of the mass-selected dication $C_7H_8^{2+}$ with xenon, where the pressure of the neutral reagent was deliberately increased to allow multicollisional processes. Due to the fact that we have recently described in detail the reactions of xenon with the $C_7H_n^{2+}$ dications (n = 6, 8) from toluene,[23] here we limit ourselves to a brief summary of the various product channels observed:

Neutral loss $C_7H_8^{2+} \rightarrow C_7H_6^{2+} + H_2$ (1)

Coulomb explosion $C_7H_8^{2+} \rightarrow C_5H_5^+ + C_2H_3^+$ (2)

$C_7H_8^{2+} \rightarrow C_4H_5^+ + C_3H_3^+$ (3)

Electron transfer $C_7H_8^{2+} + Xe \rightarrow C_7H_8^+ + Xe^+$ (4)

Dissociative el. transfer

$C_7H_8^{2+} + Xe \rightarrow C_7H_7^+ + H + Xe^+$ (5)

$C_7H_8^{2+} + Xe \rightarrow C_6H_5^+ + CH_3 + Xe^+$ (6)

Proton transfer $C_7H_8^{2+} + Xe \rightarrow C_7H_7^+ + XeH^+$ (7)

C–Xe bond formation $C_7H_8^{2+} + Xe \rightarrow C_7H_6Xe^{2+} + H_2$ (8)

Thus, the major reactions observed can be classified as (i) dissociation of metastable $C_7H_8^{2+}$ dications to afford $C_7H_6^{2+}$ concomitant with loss of H_2 according to reaction (1); (ii) charge separation reactions (“Coulomb explosions”) of the parent dication into pairs of singly charged products according to reactions (2) and (3); (iii) non-dissociative transfer of one electron from Xe to the dication according to reaction (4); (iv) transfer of one electron from Xe to the dication resulting in fragmentation of the resulting singly charged ion, *e.g.* affording the fragments $C_7H_7^+$ and $C_6H_5^+$ *via* reactions (5) and (6); (v) proton transfer from $C_7H_8^{2+}$ to xenon according to reaction (7); and (vi) formation of an organoxenon dication *via* reaction (8).

The dependence of product ion abundances on the nominal collision energy can provide additional mechanistic insight. Products of exothermic or thermoneutral reactions generally have an onset at a similar energy to that of the parent ion and peak at low collision energies, while endothermic channels require some excess energy to occur and thus peak at higher collision energies. The abundance curves as a function of collision energy for $C_7H_7^+$, $C_7H_8^+$, $C_7H_6Xe^{2+}$, Xe^+ and XeH^+, respectively, have very similar shapes with a behavior characteristic of exothermic or thermoneutral ion/molecule reactions *via* an intimate collision complex, whereas products such as $C_5H_3^+$, $C_6H_5^+$, $C_7H_5^+$ and $C_7H_6^+$ show markedly higher thresholds, clearly assigning them as the result of endothermic processes (see Fig. S1 in the ESI†).

Of interest in the context of the generation of $C_7H_6Xe^{2+}$ is the mechanism of its formation. Thus, the organoxenon dication could either be formed by an initial loss of H_2 from the dication, followed by association of the resulting $C_7H_6^{2+}$ fragment with xenon or *via* a direct exchange of H_2 by Xe in an intimate collision complex. In order to address this point, we have *inter alia* studied the pressure dependence of the various product channels. From the data in Fig. 5 it becomes obvious that the formation of $C_7H_6Xe^{2+}$ occurs as a termolecular process and is hence favored at elevated pressures, such that the rare-gas adduct is formed in a “bath of xenon”.[23]

Similarly to $C_7H_8^{2+}$, the hydrogen-depleted dication $C_7H_6^{2+}$ undergoes a bond forming reaction with xenon to afford $C_7H_6Xe^{2+}$ (see a typical mass spectrum in Fig. S2, ESI†). The abundances of the major products $C_7H_6^+$, $C_7H_5^+$,

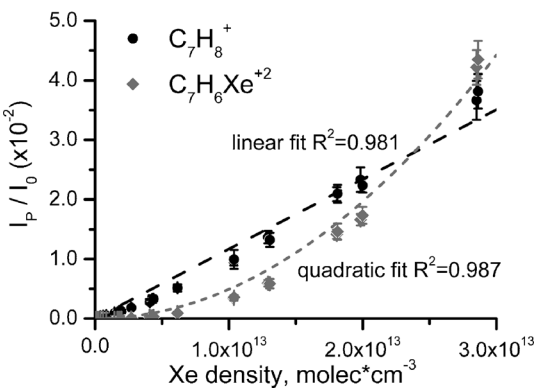

Fig. 5 Pressure dependence of two representative products, namely $C_7H_8^+$ (circles) and $C_7H_6Xe^{2+}$ (diamonds), in the reaction of the mass-selected $C_7H_8^{2+}$ dication generated from dissociative electron ionization of CHT with xenon. The dashed lines are best fit of the experimental data.

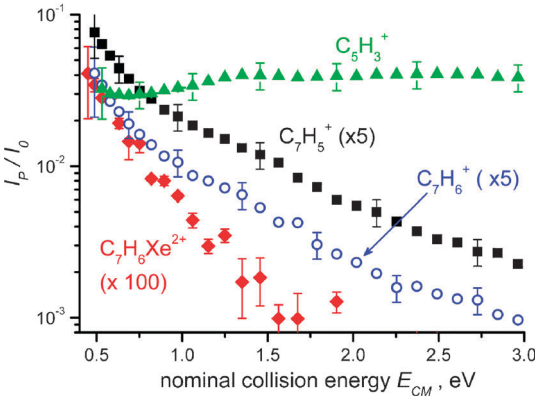

Fig. 6 Ratio of product to parent ion yields (I_P/I_0) as a function of the nominal collision energy for product ions $C_7H_6Xe^{2+}$ (filled diamonds), $C_7H_6^+$ (open circles), $C_7H_5^+$ (filled squares) and $C_5H_3^+$ (filled triangles) deriving from the reaction of $C_7H_6^{2+}$ with Xe. Below about E_{CM} = 0.5 eV, the ratio I_P/I_0 is intrinsically affected by large errors due to the reduced intensity of the primary beam as a consequence of the retarding field.

$C_5H_3^+$ and $C_7H_6Xe^{2+}$ deriving from the reactions of $C_7H_6^{2+}$ with Xe:

Coulomb explosion $C_7H_6^{2+} \rightarrow C_5H_3^+ + C_2H_3^+$ (9)

Electron transfer $C_7H_6^{2+} + Xe \rightarrow C_7H_6^+ + Xe^+$ (10)

Dissociative el. transfer $C_7H_6^{2+} + Xe \rightarrow C_7H_5^+ + H + Xe^+$ (11)

Proton transfer $C_7H_6^{2+} + Xe \rightarrow C_7H_5^+ + XeH^+$ (12)

C–Xe bond formation $C_7H_6^{2+} + Xe \rightarrow C_7H_6Xe^{2+}$ (13)

have been studied as a function of the nominal collision energy and results are shown in Fig. 6 up to E_{CM} = 3 eV. Because the data are collected using a rather high pressure of Xe in the scattering cell (about 1.6×10^{-3} mbar), secondary collisions are operative for the stabilization of collision complexes, while the secondary reactions can also draw flux from the monitored channels. Under such conditions the ratio between products and parent ion yields I_P/I_0 is no longer proportional to the cross section, but it depends on the gas pressure in the scattering cell. Therefore a pressure-dependent effective value of the cross section is derived rather than a bimolecular cross section.[56] The resulting I_P/I_0 curves for channels leading to the ionic products $C_7H_6^+$, $C_7H_5^+$ and the bond forming channel ($C_7H_6Xe^{2+}$) have similar collision energy dependences, decreasing monotonically with the increase of E_{CM} at the higher energies, with a behavior that is characteristic of exothermic or thermoneutral ion/molecule reactions. However the rate of decrease of I_P/I_0 with increasing energy is steeper for the bond-forming association channel than for the electron transfer/proton transfer channels, indicative of the fact that stabilization of the association product by a third party collision is no longer efficient when the collision energy exceeds certain values. In contrast, the curve for the monocation $C_5H_3^+$ due to Coulomb explosion of the parent dication shows a minimum at the lowest energies and a positive energy dependence in the region 0.5–1.4 eV, flattening out at the highest energies. It therefore appears as a collisionally-driven product channel, as expected due to the presence of a barrier for charge separation in the dication.

3.3 Reactive monitoring using photoionization

The formation of the $C_7H_6Xe^{2+}$ product from the reactions of $C_7H_8^{2+}$ and $C_7H_6^{2+}$ with xenon has been studied using the methodology of reactive monitoring with synchrotron radiation.[11,13,23,29–31] In such an experiment, the formation of a specific product ion from a given pair of reactants is monitored in a tandem mass spectrometer as a function of the energy of photons which are used to generate the ionic precursors. A fundamental aspect of reactive monitoring is that all parameters possibly affecting the reactivity (*e.g.* mass selection, nominal collision energy, neutral gas pressure in the reaction cell) are kept constant while the energy of the ionizing photon is scanned. Accordingly, any differences in the appearance energy of ionic products and in the shape of the photoion curves for the various product ions should be ascribed exclusively to the effect of changing the internal energy of the reacting dication due to the change in the energy of the ionizing photons. We note, in passing, that this particular kind of experiment can by and large only be performed using synchrotron radiation due to both the vacuum-UV light being required and the rapid wavelength tunability that is necessary.

Results from the reactive monitoring experiments, carried out by selecting $C_7H_8^{2+}$ as precursor dications from CHT, are shown in Fig. 7. Like in Fig. 2 (see above), the $C_7H_8^{2+}$ parent ion shows an appearance energy at 22.67 eV, while dehydrogenation to $C_7H_6^{2+}$ starts to appear at about 1 eV higher photon energy. The threshold of $C_7H_6Xe^{2+}$, as the product of particular interest, is clearly in between that of $C_7H_8^{2+}$ and $C_7H_6^{2+}$. For estimation of the energy difference between the threshold of parent and that of the $C_7H_6Xe^{2+}$ product dication, we follow the same method already applied above and shift a best fit of the data for the parent ion linearly

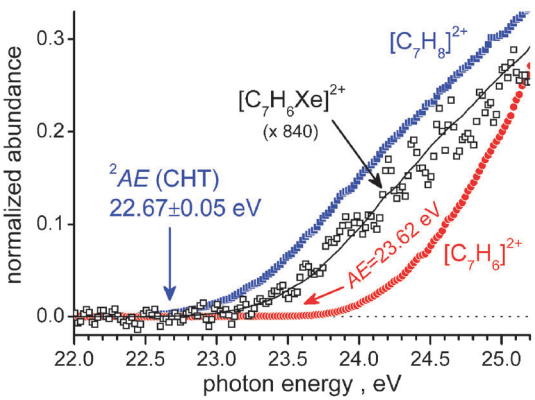

Fig. 7 Yields of the parent $C_7H_8^{2+}$ (filled squares) and product $C_7H_6Xe^{2+}$ ions (open squares) formed in the reaction of mass-selected $C_7H_8^{2+}$ with Xe as a function of the energy of the photons used for the double ionization of CHT. Photo-ion yields are also shown for the unimolecular dehydrogenation product $C_7H_6^{2+}$ (filled circles). In the case of $C_7H_6Xe^{2+}$ products the solid line represents a connection of the data points for the parent dication shifted up in energy by 0.3 eV.

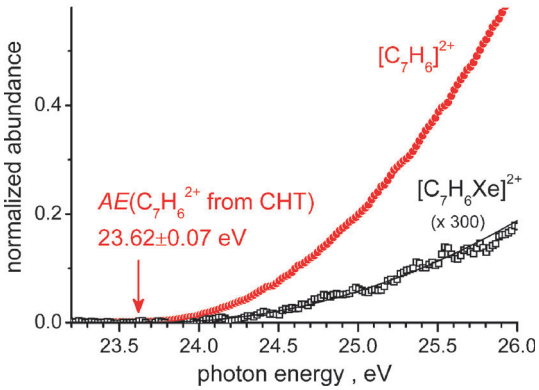

Fig. 8 Yields of the precursor dication $C_7H_6^{2+}$ (filled circles) and of the association product $C_7H_6Xe^{2+}$ (open squares) formed in the reaction of mass-selected $C_7H_6^{2+}$ with Xe as a function of the energy of the photons used for the dissociative double ionization of CHT. In the case of $C_7H_6Xe^{2+}$ the solid line is that of $C_7H_6^{2+}$ multiplied by 0.3 to indicate that the product $C_7H_6Xe^{2+}$ appears at the same photon energy as the $C_7H_6^{2+}$ reagent dication.

upwards in energy until a reasonable agreement with the experimental data for $C_7H_6Xe^{2+}$ is achieved. An upward shift of 0.3 ± 0.1 eV (solid line in Fig. 7) is in a reasonably good accord with the experimental data, thus leading to $AE(C_7H_6Xe^{2+})_{CHT}$ = (23.0 ± 0.1) eV. Similarly to the reactivity of $C_7H_8^{2+}$ generated from the toluene precursor,[23] the fact that the threshold of $C_7H_6Xe^{2+}$ is in-between those of $C_7H_8^{2+}$ and $C_7H_6^{2+}$ is an unequivocal demonstration that Xe binding to the parent dication and H_2 elimination occur in a single reaction step. The previous computational studies of the $C_7H_8^{2+}$ + Xe potential-energy surface suggest an endothermicity of 0.68 eV for the formation of $C_7H_6Xe^{2+}$ + H_2 from the CHT dication and xenon.[23] In conjunction with ^2IE(CHT) = (21.6 ± 0.2) eV, this would imply an $AE(C_7H_6Xe^{2+})_{CHT}$ of only about 22.3 eV, thus suggesting that the formation of $C_7H_6Xe^{2+}$ from the CHT dication and xenon is subject to kinetic control due to the existence of a reaction barrier. In addition, cooling of intermediate $C_7H_8Xe^{2+}$ under termolecular collision conditions could also lead to an upward shift of $AE(C_7H_6Xe^{2+})_{CHT}$. Notable in comparison with the toluene case is also the much lower yield of the organoxenon dication product from the reaction of $C_7H_8^{2+}$ from CHT, which can be attributed to the high internal energy content of the dication formed *via* vertical photoionization of the neutral compound (see above).

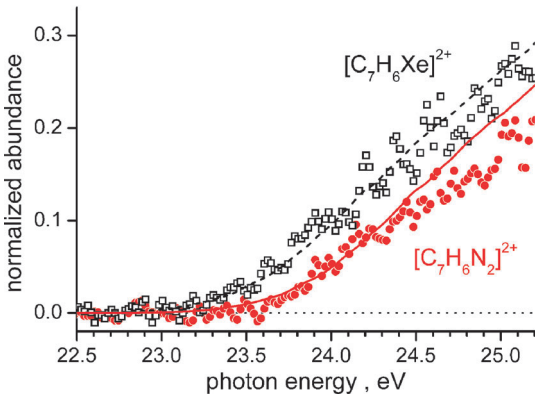

Fig. 9 Yields of the product ions $C_7H_6Xe^{2+}$ (open squares) and $C_7H_6N_2^{2+}$ (filled circles) formed in the reaction of mass-selected $C_7H_8^{2+}$ dications with Xe and N_2, respectively, as a function of the energy of photons used for the double ionization of CHT in the ion source. In the case of $C_7H_6Xe^{2+}$ products the dashed line is the same as Fig. 7, while for $C_7H_6N_2^{2+}$ the solid line is a fit of the data points for the parent dication upward shifted in energy by (0.6 ± 0.2) eV.

The results of the corresponding experiment with $C_7H_6^{2+}$ as the reactant are shown in Fig. 8. In this case, the threshold for the association product $C_7H_6Xe^{2+}$ coincides with the threshold for dissociative photoionization of CHT to the $C_7H_6^{2+}$ dication, thus indicating the absence of a barrier, as expected in the case of a pure association reaction.

In addition to xenon, we have also briefly studied the reactions of $C_7H_8^{2+}$ and $C_7H_6^{2+}$ with nitrogen using the reactive monitoring technique. Similar to the reaction with xenon, the formation of a $C_7H_6N_2^{2+}$ product is observed in the case of $C_7H_8^{2+}$ (Fig. 9), but the apparent threshold is about 0.3 eV higher in energy than in the xenon case, *i.e.* $AE(C_7H_6N_2^{2+})_{CHT}$ = (23.3 ± 0.2) eV, but yet smaller than the appearance energy of the dehydrogenation product $C_7H_6^{2+}$. This result demonstrates that also the binding of N_2 and elimination of H_2 occur in a single reaction step. When instead the hydrogen-depleted $C_7H_6^{2+}$ dication is used as a precursor, the threshold for the association product $C_7H_6N_2^{2+}$ appears at the same photon energy as the $C_7H_6^{2+}$ reagent dication, fully consistent with formation of the ion *via* termolecular ion-neutral association (Fig. S3, ESI†). These reactions of nitrogen are of potential interest with regard to the role of hydrocarbon dications in the chemistry of the ionosphere of Titan,[11–14,57] whose atmosphere has nitrogen as the major component and where ambient pressures and low temperatures favor association reactions.[58–60] Adduct formation of reactive hydrocarbon dications with nitrogen could in fact act as a sink of these species restricting their influence on the overall chemistry of the ionosphere. Alternatively, such complexes could serve as a reservoir which can stabilize the dications with regard to single-electron reduction, but release them in encounters with reactive substrates (*e.g.* C–C bond formation with methane).[11,12] Consequently, the structure of these nitrogen adducts and their chemistry are currently under investigation in our laboratories.

4. Conclusions

The double photoionization of neutral cycloheptatriene (CHT) shows an unexpected behavior when we monitor the formation of the molecular dication $C_7H_8^{2+}$ and the primary fragment $C_7H_6^{2+}$, as a function of the photon energy. Analysis of the photodication appearance curves in conjunction with theoretical results implies the occurrence of a situation which is somewhat unusual for dications formed from aromatic hydrocarbons in that the adiabatic transition from the neutral ground state to the dication ground state is associated with negligible Franck–Condon factors.[61] The analysis of the data in terms of Born–Haber cycles yields a second ionization energy of ^2IE(CHT) = (21.6 ± 0.2) eV,

whereas the formal appearance energy of the dication in photoionization experiment is about 1 eV larger. The reactivity of the $C_7H_6^{2+}$ and $C_7H_8^{2+}$ dications with xenon is investigated and, among other pathways, a bond-forming channel to the organoxenon dication $C_7H_6Xe^{2+}$ is observed. The mechanism of the reaction is studied by reactive monitoring with synchrotron radiation which is an interesting technique for mapping out the energy landscape of reactive dications. In collisions with N_2 the $C_7H_6N_2^{2+}$ adduct is observed, which suggests that such species may also exist in the higher layers of extraterrestrial, nitrogen-rich atmospheres.

Acknowledgements

This work was supported by the Academy of Sciences of the Czech Republic (Z40550506), the European Research Council (AdG HORIZOMS), the Grant Agency of the Czech Republic (203/09/1223 and P208/11/0446), the Ministry of Education of the Czech Republic (MSM0021620857, OC10046), the University of Trento. JA gratefully acknowledges a PhD fellowship from the "Fondazione Trentino-Università". The synchrotron measurements at SOLEIL were supported by the ELISA framework and we thank the DESIRS beamline manager Dr L. Nahon and his team for assistance during the measurements and the technical staff of SOLEIL for running the facility.

References

1 P. Scheier, in *Encyclopedia of Mass Spectrometry*, ed. P. B. Armentrout, Elsevier, Amsterdam, 2003, vol. 1, p. 455.
2 J. Roithová, Z. Herman, D. Schröder and H. Schwarz, *Chem.–Eur. J.*, 2006, **12**, 2465.
3 S. A. Rodgers, S. D. Price and S. R. Leone, *J. Chem. Phys.*, 1993, **98**, 280.
4 S. D. Price, M. Manning and S. R. Leone, *J. Am. Chem. Soc.*, 1994, **116**, 8673.
5 S. D. Price, *Phys. Chem. Chem. Phys.*, 2003, **5**, 1717.
6 J. Roithová and D. Schröder, *J. Am. Chem. Soc.*, 2006, **128**, 4208.
7 J. Roithová and D. Schröder, *Chem.–Eur. J.*, 2007, **13**, 2893.
8 J. Roithová and D. Schröder, *Phys. Chem. Chem. Phys.*, 2007, **9**, 731.
9 P. Milko, J. Roithová, D. Schröder and H. Schwarz, *Int. J. Mass Spectrom.*, 2007, **267**, 139.
10 J. Roithová and D. Schröder, *Phys. Chem. Chem. Phys.*, 2007, **9**, 731.
11 C. L. Ricketts, D. Schröder, C. Alcaraz and J. Roithová, *Chem.–Eur. J.*, 2008, **14**, 4779.
12 J. Roithová, C. L. Ricketts and D. Schröder, *Int. J. Mass Spectrom.*, 2009, **280**, 32.
13 D. Ascenzi, J. Roithová, D. Schröder, E.-L. Zins and C. Alcaraz, *J. Phys. Chem. A*, 2009, **113**, 11204.
14 E. L. Zins and D. Schröder, *J. Phys. Chem. A*, 2010, **114**, 5989.
15 Review: J. Roithová and D. Schröder, *Phys. Chem. Chem. Phys.*, 2007, **9**, 2341.
16 J. Roithová, C. L. Ricketts, D. Schröder and S. D. Price, *Angew. Chem., Int. Ed.*, 2007, **46**, 9316.
17 J. Roithová, H. Schwarz and D. Schröder, *Chem.–Eur. J.*, 2009, **15**, 9995.
18 D. Ascenzi, P. Tosi, J. Roithová and D. Schröder, *Chem. Commun.*, 2008, 4055.
19 D. Ascenzi, P. Tosi, J. Roithová, C. L. Ricketts, D. Schröder, J. F. Lockyear, M. A. Parkes and S. D. Price, *Phys. Chem. Chem. Phys.*, 2008, **10**, 7121.
20 J. Roithová and D. Schröder, *Angew. Chem., Int. Ed.*, 2009, **48**, 8788.
21 J. F. Lockyear, K. Douglas, S. D. Price, M. Karwowska, K. Fijałkowski, W. Grochala, M. Remeš, J. Roithová and D. Schröder, *J. Phys. Chem. Lett.*, 2010, **1**, 358.
22 E.-L. Zins and D. Schröder, *Int. J. Mass Spectrom.*, 2011, **299**, 53.
23 E.-L. Zins, P. Milko, D. Schröder, J. Aysina, D. Ascenzi, J. Žabka, C. Alcaraz, S. D. Price and J. Roithová, *Chem.–Eur. J.*, 2011, **17**, 4012.
24 J. Roithová, D. Schröder, J. Loos, H. Schwarz, H.-C. Jankowiak, R. Berger, R. Thissen and O. Dutuit, *J. Chem. Phys.*, 2005, **122**, 094306.
25 J. Roithová, D. Schröder, P. Grüne, T. Weiske and H. Schwarz, *J. Phys. Chem. A*, 2006, **110**, 2970.
26 O. Dutuit, in *Fundamentals of Gas Phase Ion Chemistry*, ed. K. R. Jennings, Kluwer, Amsterdam, 1991, p. 21.
27 O. Dutuit, C. Alcaraz, D. Gerlich, P. M. Guyon, J. W. Hepburn, C. Métayer-Zeitoun, J. B. Ozenne, M. Schweizer and T. Weng, *Chem. Phys.*, 1996, **209**, 177.
28 C. Alcaraz, C. Nicolas, R. Thissen, J. Žabka and O. Dutuit, *J. Phys. Chem. A*, 2004, **108**, 9998.
29 D. Schröder, J. Loos, H. Schwarz, R. Thissen, O. Dutuit, P. Mourgues and H.-E. Audier, *Angew. Chem., Int. Ed.*, 2002, **41**, 2748.
30 D. Schröder, J. Loos, H. Schwarz, R. Thissen and O. Dutuit, *J. Phys. Chem. A*, 2004, **108**, 9931.
31 J. Roithová and D. Schröder, *Chem. Listy*, 2009, **103**, 636.
32 D. Ascenzi, N. Cont, G. Guella, P. Franceschi and P. Tosi, *J. Phys. Chem. A*, 2007, **111**, 12513.
33 D. Ascenzi, D. Bassi, P. Franceschi, P. Tosi, M. Di Stefano, M. Rosi and A. Sgamellotti, *J. Chem. Phys.*, 2003, **119**, 8366 and references therein.
34 S. H. Vosko, L. Wilk and M. Nusair, *Can. J. Phys.*, 1980, **58**, 1200.
35 C. Lee, W. Yang and R. G. Parr, *Phys. Rev. B*, 1988, **37**, 785.
36 B. Miehlich, A. Savin, H. Stoll and H. Preuss, *Chem. Phys. Lett.*, 1989, **157**, 200.
37 A. D. Becke, *J. Chem. Phys.*, 1993, **98**, 5648.
38 N. Godbout, D. R. Salahub, J. Andzelm and E. Wimmer, *Can. J. Chem.*, 1992, **70**, 560.
39 F. Blanco, M. Solimannejad, I. Alkorta and J. Elguero, *Theor. Chem. Acc.*, 2008, **121**, 181.
40 M. J. Frisch, G. W. Trucks, H. B. Schlegel, G. E. Scuseria, M. A. Robb, J. R. Cheeseman, J. A. Montgomery, Jr, T. Vreven, K. N. Kudin, J. C. Burant, J. M. Millam, S. S. Iyengar, J. Tomasi, V. Barone, B. Mennucci, M. Cossi, G. Scalmani, N. Rega, G. A. Petersson, H. Nakatsuji, M. Hada, M. Ehara, K. Toyota, R. Fukuda, J. Hasegawa, M. Ishida, T. Nakajima, Y. Honda, O. Kitao, H. Nakai, M. Klene, X. Li, J. E. Knox, H. P. Hratchian, J. B. Cross, C. Adamo, J. Jaramillo, R. Gomperts, R. E. Stratmann, O. Yazyev, A. J. Austin, R. Cammi, C. Pomelli, J. W. Ochterski, P. Y. Ayala, K. Morokuma, G. A. Voth, P. Salvador, J. J. Dannenberg, V. G. Zakrzewski, S. Dapprich, A. D. Daniels, M. C. Strain, O. Farkas, D. K. Malick, A. D. Rabuck, K. Raghavachari, J. B. Foresman, J. V. Ortiz, Q. Cui, A. G. Baboul, S. Clifford, J. Cioslowski, B. B. Stefanov, G. Liu, A. Liashenko, P. Piskorz, I. Komaromi, R. L. Martin, D. J. Fox, T. Keith, M. A. Al-Laham, C. Y. Peng, A. Nanayakkara, M. Challacombe, P. M. W. Gill, B. Johnson, W. Chen, M. W. Wong, C. Gonzalez and J. A. Pople, *GAUSSIAN 03 (Revision C.02)*, Gaussian, Inc., Wallingford CT, 2004.
41 C. Gonzalez and H. B. Schlegel, *J. Chem. Phys.*, 1989, **90**, 2154.
42 C. Gonzalez and H. B. Schlegel, *J. Phys. Chem.*, 1990, **94**, 5523.
43 R. D. Molloy and J. H. D. Eland, *Chem. Phys. Lett.*, 2006, **421**, 31.
44 J. Roithová, J. Žabka, D. Ascenzi, P. Franceschi, C. L. Ricketts and D. Schröder, *Chem. Phys. Lett.*, 2006, **423**, 254.
45 P. Milko, D. Schröder, K. Lemr, J. Žabka, C. Alcaraz and J. Roithová, *Collect. Czech. Chem. Commun.*, 2009, **74**, 101.
46 G. H. Wannier, *Phys. Rev.*, 1953, **90**, 817.
47 G. H. Wannier, *Phys. Rev.*, 1955, **100**, 1180.
48 S. Geltman, *Phys. Rev.*, 1956, **102**, 171.
49 U. Fano, *Rep. Prog. Phys.*, 1983, **46**, 97.
50 M. S. Lubell, *Z. Phys. D: At., Mol. Clusters*, 1994, **30**, 79.
51 C. L. Ricketts, D. Schröder, J. Roithová, H. Schwarz, R. Thissen, O. Dutuit, J. Žabka, Z. Herman and S. D. Price, *Phys. Chem. Chem. Phys.*, 2008, **10**, 5135.
52 H. Kossmann, V. Schmidt and T. Andersen, *Phys. Rev. Lett.*, 1988, **60**, 1266.

53 J. R. Friedman, X. Q. Guo, M. S. Lubell and M. R. Frankel, *Phys. Rev. A*, 1992, **46**, 652.
54 The notation $C_7H_6^{2+}{}_{Tol}$ is used to refer to the $C_7H_6^{2+}$ dication originating from neutral toluene.
55 Data for the neutral and monocationic compounds are taken from: NIST Chemistry Webbook, National Institute of Standards and Technology, Gaithersburg, USA, see: http://webbook.nist.gov/chemistry/.
56 D. Ascenzi, D. Bassi, P. Franceschi, O. Hadjar, P. Tosi, M. Di Stefano, M. Rosi and A. Sgamellotti, *J. Chem. Phys.*, 2004, **121**, 6728.
57 S. Miller, J. I. Moses, S. J. Klippenstein, J. M. C. Plane, R. V. Yelle, S. K. Atreya, D. F. Strobel, S. D. Le Picard, I. R. Sims, P. Casavecchia, A. Suits, P. W. Seakins, A. Faure, Y. Ellinger, N. Mason, P. Pernot, B. Bezard, C. Manzanares, R. I. Kaiser, V. Vuitton, M. Meuwly, T. S. Zwier, M. Dobrijevic, R. Thissen, N. G. Adams, L. Biennier, M. Ashfold, A. M. Mebel, D. Schram, J. B. Mitchell, J.-C. Loison and S. Lutz, *Faraday Discuss.*, 2010, **147**, 251.
58 J. Žabka, M. Polášek, D. Ascenzi, P. Tosi, J. Roithová and D. Schröder, *J. Phys. Chem. A*, 2009, **113**, 11153.
59 N. G. Adams, L. D. Mathews and D. Osborne Jr, *Faraday Discuss.*, 2010, **147**, 323.
60 D. Ascenzi, J. Aysina, P. Tosi, A. Maranzana and G. Tonachini, *J. Chem. Phys.*, 2010, **133**, 184308.
61 For single ionization of ammonia as a related, but less extreme example, see: A. Peluso, R. Borrelli and A. Capobianco, *J. Phys. Chem. A*, 2009, **113**, 14831.

